Journal of Food and Drug Analysis

Volume 31 | Issue 2 Article 13

Using lanthanide ions as magnetic and sensing probes for the detection of Tetracycline from complex samples

ORIGINAL ARTICLE

Using lanthanide ions as magnetic and sensing probes for the detection of tetracycline from complex samples

Yan-Cen Zhan [a], Chin-Poa Chiu [a], Yu-Chie Chen [a,b,*]

[a] Department of Applied Chemistry, National Yang Ming Chiao Tung University, Hsinchu 300, Taiwan
[b] International College of Semiconductor Technology, National Yang Ming Chiao Tung University, Hsinchu 300, Taiwan

Abstract

Tetracycline (TC) is a broad-spectrum antibiotic and has been added to animal feeds to grow livestock under healthy conditions, making it important to have effective methods for rapidly detecting TC in complex samples. In this study, a novel method that uses lanthanide ions (i.e. Eu^{3+} and Gd^{3+}) as magnetic and sensing probes for the detection of TC from aqueous samples is explored. When dissolving Gd^{3+} in tris(hydroxymethyl)aminomethane (Tris) buffer at pH 9, magnetic Gd^{3+}-Tris conjugates can be readily generated. The magnetic Gd^{3+}-Tris conjugates possess trapping capacity toward TC from sample solutions via the chelation of Gd^{3+} and TC. Eu^{3+} is used as the fluorescence sensing probe against TC on the Gd^{3+}-TC conjugates via the antenna effect. The fluorescence response derived from Eu^{3+} is increased with the increase of TC trapped on the Gd^{3+}-based probes. The linear dynamic range against TC ranges from 20 to 320 nM, whereas the limit of detection toward TC is ~2 nM. Furthermore, the developed sensing method can be employed for the visual assay of TC with a concentration above ~0.16 μM under UV light illumination in the dark. Furthermore, we have demonstrated the applicability of the developed method to quantify TC in a chicken broth sample with complex matrix. Our developed method offers several advantages, including high sensitivity and good selectivity, for the detection of TC in complex samples.

Keywords: Antenna effect, Eu^{3+}, Gd^{3+}, Magnetic probes, Tetracycline

1. Introduction

Since the discovery of tetracycline (TC) in the 1940s [1], TC has been extensively used in the medical treatment of bacterial infections [2]. TC is a broad-spectrum antibiotic. Thus, it has been applied in veterinary medicine and added to animal feeds to gain good profit [3]. However, the discharge of TC-containing waste water and materials to sewage or land can cause environmental pollution [4]. In addition, TC residues have been frequently found in wastewater, surface water, groundwater, and soil [4]. Moreover, the overuse of TC has raised a public health concern. Various pathogenic bacteria have become TC-resistance strains [2,5]. The accumulation of TC in human bodies can bring adverse impacts such as allergic reactions, endocrine disruption [6], and chronic toxicity [7]. Thus, the European Union has suggested the maximum residue limits (MRL) for milk and chicken meat (MRL: 0.1 mg kg^{-1}) and eggs (MRL: 0.2 mg kg^{-1}) [8,9].

High-performance liquid chromatography [10], liquid chromatography-mass spectrometry [11], chemiluminescence [12], and fluorometry [13–15] are common techniques which are developed to separate, analyze, and quantify TC. Among these techniques, fluorescence-based detection approaches provide superior features including simplicity, high sensitivity, and rapid response [14,16]. Quantum dots [17], metal-organic frameworks [18], and nanomaterials [19] have been explored to be suitable fluorescence-sensing probes for the detection of TC from complex samples. However, the matrix from complex samples can cause an autofluorescence background and affect the detection of TC [16]. Thus, sample pretreatments are often applied before detection to improve the sensitivity and selectivity of the sensing methods toward TC [20,21].

Received 26 January 2023; accepted 21 May 2023.
Available online 15 June 2023

* Corresponding author at: Department of Applied Chemistry, National Yang Ming Chiao Tung University, Hsinchu 300, Taiwan. Fax: +886 3 5173764.
E-mail address: yuchie@nycu.edu.tw (Y.-C. Chen).

https://doi.org/10.38212/2224-6614.3457

Enrichment is a common strategy that is used in sample pretreatment for concentrating trace target analytes and the elimination of unwanted species from complex samples [22,23]. Magnetic probes that can be used to effectively concentrate TC from complex samples have also been demonstrated [24–26]. The main advantage of using magnetic probes in the sample pretreatment is that the target analytes trapped by the magnetic probes can be easily isolated by applying an external magnet for a short period [26,27]. Nevertheless, the fabrication and functionalization of magnetic probes often require at least several hours [24,25]. Thus, the simplification of the generation of functional probes with magnetic properties is anticipated. Recently, we have demonstrated that bacteria and cells can acquire magnetism by using magnetic metal ions as the trapping probe [28,29]. Magnetic metal ions (e.g., Gd^{3+}, Co^{2+}, Fe^{3+}, and Ni^{2+}) alone in the aqueous solution have no visible magnetism when applying an external magnet. However, magnetic conjugates containing magnetic metal ions and their target analytes such as mammalian cells and bacteria had visible and manipulable magnetism when applying an external magnet [29,28]. It was because a high density of magnetic metal ions aggregated in a small space using cells and bacteria as the interface, leading to an enhanced magnetism strength [29,28]. In such approaches, the time required to synthesize magnetic probes was eliminated, whereas these selected magnetic metal ions had a specific binding affinity toward their target species. The affinity between those target species with magnetic metal ions resulted from the favorable binding of the functional groups on the target species and magnetic metal ions [29,28]. For example, Gd^{3+} has been recognized as a hard acid according to the theory of Hard and Soft Acids and Bases (HSAB) [30]. Thus, it should have a good binding affinity with hard bases such as TC which contains several ketone functional groups. Thus, we believe that Gd^{3+} can be used as the magnetic probe against TC from complex samples. Moreover, TC can absorb the excitation energy and transfer the energy to Eu^{3+} because of the antenna effect [31–34]. Therefore, the fluorescence derived from Eu^{3+} can be further enhanced when complexing with TC [31,32]. Thus, Eu^{3+} was added to the resultant Gd^{3+}-TC conjugates as the fluorescence sensing probes in this study. Chicken broth extract was used as the model sample to demonstrate the practice of using our method for the rapid characterization of TC in real world samples.

2. Experimental section

Materials, chemicals, and instruments used in this work are described in Support Information.

2.1. Generation of the Gd^{3+}-Tris conjugates

Heating samples under microwave-heating is an efficient means to reduce incubation time in trapping and enrichment [33]. Thus, the generation of the Gd^{3+}-Tris conjugates was conducted under microwave-heating. Aqueous $GdCl_3$ (0.4 M) was prepared in Tris buffer (10 mM) at pH 9. Subsequently, NaOH (2N, 4 μL) was added into the aqueous $GdCl_3$ (0.4 M, 0.3 mL) that had been placed in a water bath (3 mL). The mixture was incubated in a microwave-oven (180 W, 2.5 min × 2). The resultant sample was placed next to a magnet for 30 min. The magnetic Gd^{3+}-Tris aggregates were then collected by removing the supernatant (0.27 mL). The resultant Gd^{3+}-Tris conjugates were rinsed by Tris buffer (10 mM, 0.3 mL, pH 9) and isolated by an external magnet (10 min). The rinse steps were repeated twice, and 0.3 mL of supernatant was removed during rinse steps. The resultant magnetic Gd^{3+}-Tris aggregates were used as the probes in this work. Moreover, the resultant conjugates were examined by superconducting quantum interference device magnetometer (SQUID).

2.2. Trapping and sensing TC using our developed method

All steps for using the Gd^{3+}-Tris conjugates as trapping probes toward TC followed by Eu^{3+} fluorescence sensing are summarized below. The Gd^{3+}-Tris conjugates (~2 μg μL^{-1}, 50 μL) were added to the sample (1 mL) containing TC prepared in Tris buffer (10 mM, pH 8). The resulting sample was incubated in a water bath (3 mL) followed by placing in a microwave oven (180 W, 2.5 min). The resulting sample was isolated by placing an external magnet (~4000 Gauss) next to the same vial for 30 min. After removing the supernatant (0.98 mL), the isolated conjugates were rinsed with Tris buffer (1 mL, 10 mM, pH 8) followed by addition with aqueous Eu^{3+} (0.1 mM, 50 μL) that had been prepared in Tris buffer (80 mM) at pH 8. The mixture was placed in a water bath (400 mL) at 45 °C for 15 min. After 15 min, the samples were analyzed by fluorescence spectroscopy.

2.3. Naked eye detection

Our approach allowed us to visualize the results of the sample containing TC above a certain concentration with adjusted concentrations and volumes of the Gd^{3+}-Tris conjugates and Eu^{3+} under the illumination of UV light in the dark. Samples (1 mL) containing TC (0.08–10.00 μM) added with the Gd^{3+}-Tris conjugates (10 μg μL^{-1}, 20 μL) were examined. Aqueous Eu^{3+} (4 mM, 0.1 mL) was added to the sample after the magnetic Gd^{3+}-TC conjugates were formed. Otherwise, the experimental steps were similar to those stated in the previous section. The photographs of the resulting samples were taken with a camera under UV lamp illumination (λ_{max} = 365 nm).

3. Results and discussion

3.1. Characterization of the Gd^{3+}-Tris conjugates

The generated Gd^{3+}-Tris conjugates possessed visible magnetism and could be aggregated by placing an external magnet (inset in Fig. 1). White precipitates resulting from the Gd^{3+}-Tris conjugates were attracted to the wall by an external magnet that was placed on the left-hand side of the bottle. Fig. 1 shows its corresponding hysteresis curves obtained at 10 (black) and 298 K (red). The magnetic susceptibilities of the conjugates were 2.06 × 10^{-3} and 9.62 × 10^{-5} emu g^{-1} at 10 and 298 K, respectively, based on the slopes of the hysteresis curves. Although the susceptibility of the conjugates was only 9.62 × 10^{-5} emu g^{-1} at 298 K, it was high enough to magnetically isolate the conjugates by an external magnet.

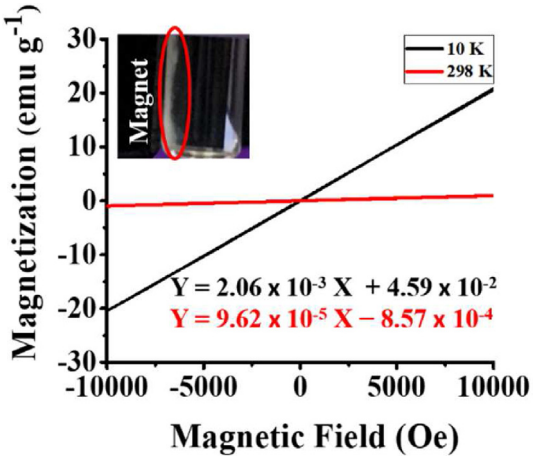

Fig. 1. Hysteresis curves of the Gd^{3+}-Tris conjugates obtained at 298 K (red) and 10 K (black). Inset photograph shows the conjugates were aggregated on the wall next to a magnet (~4000 Gauss). The circled part shows where the magnetic conjugates are.

3.2. Using the magnetic Gd^{3+}-Tris conjugates as probes for trapping TC

Based on the HSAB theory, the hard-acid Gd^{3+} should exhibit good affinity toward the hard-base TC, which possesses N- and O-containing functional groups. The feasibility of using our magnetic probes compose of the Gd^{3+}-Tris conjugates for trapping TC was examined. The photographs of the Gd^{3+}-Tris conjugate without (left) and with (right) placing an external magnet next to the bottles were shown in Fig. 2A. The white aggregates were attracted to the wall of the bottle by an external magnet. Fig. 2B displays the pictures of the samples containing TC at a high concentration with the addition of our probes obtained before (left) and after (right) magnetic isolation. The pale-yellow solution and yellowish conjugates derived from TC and our probes settled down on the bottom of the bottle, respectively, were apparent before magnetic isolation (the left photograph in Fig. 2B). However, the solution of the sample became colorless after magnetic isolation. Moreover, the magnetic aggregates with yellow color adhered to the wall next to the magnet (right photograph in Fig. 2B). These results showed that our magnetic probes possessed the capacity to trap TC and the probe-TC conjugates could be magnetically aggregated by an external magnet.

3.3. Optimization of the trapping conditions

We employed microwave heating for the incubation of the sample with our magnetic probes to accelerate the analysis. Supporting Information (SI) Fig. S1A [https://www.jfda-online.com/cgi/viewcontent.cgi?filename=0&article=3457&context=journal&type=additional] shows the UV–Vis absorption spectra of the supernatants of the samples containing TC obtained before (black) and after incubation with our probes in a microwave oven with a power of 180 W for 1.5 (blue) and 2.5 min (pink) and vortex-mixing (30 (green) and 60 min (dark blue)) followed by magnetic isolation. SI Fig. S1B [https://www.jfda-online.com/cgi/viewcontent.cgi?filename=0&article=3457&context=journal&type=additional] shows the summarized results from SI Fig. S1A [https://www.jfda-online.com/cgi/viewcontent.cgi?filename=0&article=3457&context=journal&type=additional]. The absorption spectrum of the resultant supernatant (red) was obtained by standing the sample with the magnetic probes at room temperature with magnetic separation for 30 min. The absorption bands obtained after incubation under microwave-heating (blue and pink)

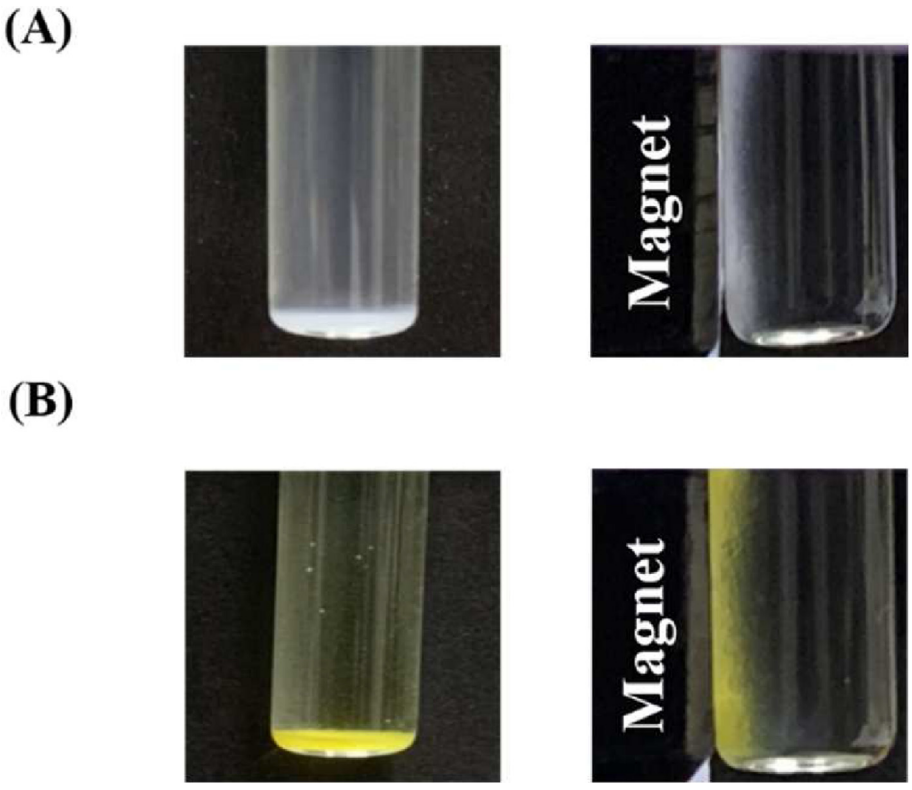

Fig. 2. Photographs of the Gd^{3+}-tris conjugates only (A) and containing TC (1 mM, 300 μL) at pH 8 (B) without (left) and with (right) placing an external magnet (~4000 Gauss) next to each vial. The photographs were taken under room light.

and vortex-mixing (green and dark blue) were much lower than that only incubated by standing at room temperature (red), indicating microwave-heating and vortex-mixing were helpful for accelerating the trapping process. Furthermore, there was a red shift at ~400 nm occurring from the samples obtained after incubation under vortex-mixing (green and dark blue). That is, the red shift resulting from the Gd^{3+}-TC conjugates, in which the Gd^{3+} was released from our probes, indicating vortex-mixing the sample and our probes too long could cause the instability of our magnetic probes. Similar phenomena have been observed when metal ions bind with TC [34]. To further confirm our suspection, we mixed TC and Gd^{3+} together to examine whether the absorption band had a red shift compared with that of TC alone. SI Fig. S2 [https://www.jfda-online.com/cgi/viewcontent.cgi?filename=0&article=3457&context=journal&type=additional] shows the absorption spectra of aqueous Gd^{3+} (black), TC (red), and the mixture (green) containing Gd^{3+} (12.8 mM) and TC (25 μM). The maximum absorption band derived from TC (red) had a red shift after adding Gd^{3+} (green), indicating that the red shift observed in SI Fig. S1A [https://www.jfda-online.com/cgi/viewcontent.cgi?filename=0&article=3457&context=journal&type=additional] was resulting from Gd^{3+} released from the conjugates of Gd^{3+}-TC. Thus, although the binding amount of TC on our magnetic probes under vortex-mixing for 30 min was a little bit more than that under microwave-heating, we selected microwave-heating for 2.5 min as the incubation method by considering the short time and stability of our magnetic probes.

3.4. Examination of the optimal pH

We then investigated the binding capacity of our magnetic probes toward TC at different pH conditions. SI Fig. S3 [https://www.jfda-online.com/cgi/viewcontent.cgi?filename=0&article=3457&context=journal&type=additional] shows the summarized results of the binding amount of the Gd^{3+} conjugates toward TC. The structure of TC is shown in the inset. The highest binding capacity, i.e. 161 ± 25 nmol mg^{-1}, was found at pH 8. Presumably, the favorable binding at pH 8 was related to the pKa value of TC (pKa_2 = 7.78) (SI Fig. S3 [https://www.jfda-online.com/cgi/viewcontent.cgi?filename=0&article=3457&context=journal&type=additional]) [35]. When the pH was around the pKa value of TC, the two chelation groups, i.e. two β-diketones, on

TC can favorably coordinate to bind with metal ions [36]. Therefore, TC on our probes has the maximum binding capacity at pH 8. Thus, pH 8 was selected as the pH for the preparation of the samples through this study.

3.5. Using Eu^{3+} as the fluorescence sensing probe

Eu^{3+} is a suitable sensing probe for detecting TC based on the antenna effect between Eu^{3+} and TC [37]. Thus, examining the feasibility of using Eu^{3+} as sensing probes against TC on our probes, some experiments were initially examined. Given that our probes were made of the Gd^{3+}-Tris conjugates, trace Gd^{3+} was unavoidably released to the supernatant during equilibrium. Thus, we examined whether the presence of Gd^{3+} in the sample containing TC using Eu^{3+} as the sensing probes would affect the sensing results. The fluorescence spectra of the samples containing TC were obtained using Eu^{3+} as the sensing probe, and the results are shown in Fig. S4 [https://www.jfda-online.com/cgi/viewcontent.cgi?filename=0&article=3457&context=journal&type=additional]. The blue curve represents the fluorescence spectrum of TC without the addition of Gd^{3+}, while the black curve corresponds to the fluorescence spectrum obtained after adding Gd^{3+} to the sample. The fluorescence spectrum in red was obtained from the control sample containing Eu^{3+} and Gd^{3+} prepared in Tris buffer (10 mM, pH 9). No emission derived from Eu^{3+} was observed without the presence of TC. However, the emission band appearing at 615 nm was observed in the fluorescence spectra (black and blue) in the presence of TC. The one with the presence of Gd^{3+} (black) had a much higher fluorescence intensity than that without Gd^{3+}. Given that Gd^{3+} has no emission at the wavelength of 615 nm, presumably that Gd^{3+} favored binding with Tris and left more vacancy available on Eu^{3+} for binding with TC.

Thus, we also examined whether the increase of the concentration of Tris in the sample might help the enhancement of the emission of Eu^{3+} in the sample containing the same concentration of TC. SI Fig. S5 [https://www.jfda-online.com/cgi/viewcontent.cgi?filename=0&article=3457&context=journal&type=additional] shows the fluorescence spectra of the samples containing TC alone (black), Eu^{3+} alone (red), Eu^{3+} mixed with Gd^{3+} (blue), Eu^{3+} mixed with TC (pink), and Gd^{3+} with TC mixed with Eu^{3+} (green) dissolved in Tris buffer at the concentrations of 10–100 mM (λ_{ex} = 397 nm). No emission was found in the spectra of the samples containing TC alone (black), Eu^{3+} alone (red), and Eu^{3+} mixed with Gd^{3+} (blue). The fluorescence intensity of Eu^{3+} with TC without (pink) and with adding Gd^{3+} (green) were compared. We found that fluorescence intensity at the wavelength of 615 nm derived from Eu^{3+} in the mixture containing TC and Eu^{3+} in the presence of Gd^{3+} enhanced the most in Tris buffer at the concentration of 80 mM. In addition, it was higher than the sample in the absence of Gd^{3+} (pink). That is, 80 mM was the optimal concentration for our subsequent experiments.

The optimal pH for the sensing experiments was further investigated. SI Fig. S6 [https://www.jfda-online.com/cgi/viewcontent.cgi?filename=0&article=3457&context=journal&type=additional] shows the fluorescence spectra of the samples containing TC with the addition of Eu^{3+} prepared in Tris buffer (10 mM) at different pH (pH 6–9). The fluorescence intensity at 615 nm derived from Eu^{3+} was the highest at pH 8. Presumably, TC and Eu^{3+} have the most favorable binding condition at pH 8 [32,36]. Then, we further employed Eu^{3+} as the sensing probe for TC trapped on our magnetic probes. Fig. 3A and B shows the photographs of the samples containing Eu^{3+} alone and our magnetic probes mixed with Eu^{3+}, respectively, with an external magnet next to each sample vial. No magnetic aggregations were observed in the sample containing Eu^{3+} alone. White precipitates (red circulated) resulting from our magnetic probes were attached to the wall next to the magnet. Fig. 3C and D shows the photographs of our magnetic probe-TC conjugates obtained before and after adding Eu^{3+}. Given that a high concentration of TC (1 mM) was present in the samples of Fig. 3C, the conjugates with pale greenish fluorescence resulting from TC were observed, thereby indicating that TC was bound to our magnetic probes. After adding Eu^{3+}, the solution became pinkish because of the formation of Eu^{3+}-TC complexes (Fig. 3D), indicating that Eu^{3+} could compete with Gd^{3+} to bind with TC on our magnetic probe-TC conjugates, thus leading to the release of TC and formation of Eu^{3+}-TC complex in the supernatant. It was also clear from the diminishing of the thick greenish conjugates attached to the wall next to the magnet. These results indicated that Eu^{3+} can be used as the sensing probe in our approach.

3.6. Examination of the optimal experimental conditions

Eu^{3+} (50 μL) with different concentrations was added to the magnetic Gd^{3+}-TC conjugates to optimize the concentration of Eu^{3+}. SI Fig. S7A–S7F [https://www.jfda-online.com/cgi/viewcontent.cgi?filename=0&article=3457&context=journal&type=additional]

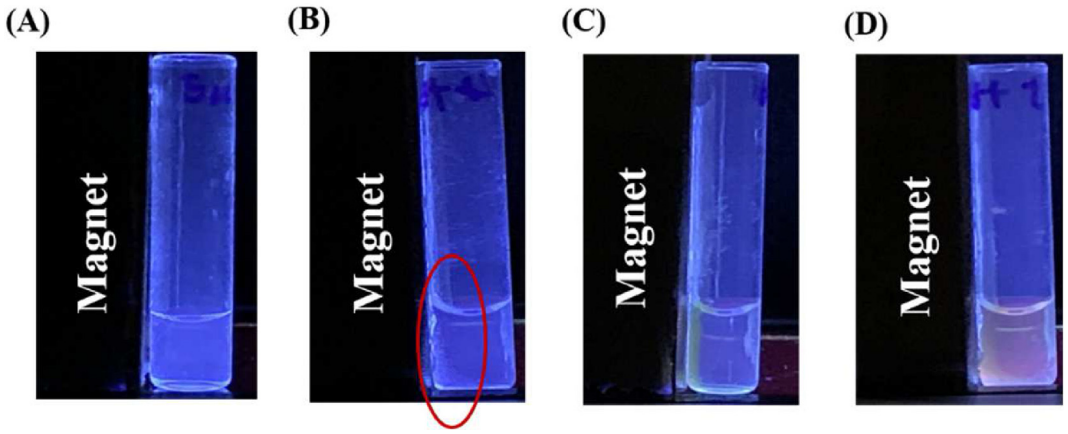

Fig. 3. Photographs of (A) Eu^{3+} only (0.05 M, 0.1 mL) and (B) our magnetic probes mixed with the same concentration of Eu^{3+}. The circulated part indicates where the magnetic conjugates are. Photographs of our magnetic probe-TC conjugates obtained (C) before and (D) after the addition of Eu^{3+}. These photographs were taken under UV light (λ = 365 nm) in the dark.

show the representative fluorescence spectra of the samples containing Eu^{3+} with different concentrations obtained after mixing with our magnetic probes with (red) and without bound with TC (black). SI Fig. S7G [https://www.jfda-online.com/cgi/viewcontent.cgi?filename=0&article=3457&context=journal&type=additional] shows the summarized bar graphs by plotting I'/I_0', where I_0' and I' stand for the peak height at 615 nm derived from Eu^{3+} obtained after mixed with the Gd^{3+}-Tris conjugates and the Gd^{3+}-Tris-TC conjugates, respectively. However, the result suggested that the intensity of Eu^{3+} at low concentrations (≤31.3 μM) was too low to be calculated accurately, thus leading to a large error. The highest enhancement of the fluorescence intensity was found when the concentration of Eu^{3+} reached 62.5 μM in the mixture. Thus, Eu^{3+} with a final concentration of 62.5 μM was used in the following studies.

The incubation time for mixing our probes with Eu^{3+} was also examined. SI Fig. S8 [https://www.jfda-online.com/cgi/viewcontent.cgi?filename=0&article=3457&context=journal&type=additional] shows the summarized results. The fluorescence intensity at 615 nm reached the maximum when the incubation time reached 15 min. When the incubation time was longer than 15 min, the fluorescence intensity slightly decreased. This was possibly because the TC was reversely bound to the probes. Therefore, 15 min was selected as the incubation time.

3.7. Quantitative analysis

To evaluate the feasibility of our method for quantitative analysis of TC, we conducted experiments using samples with different concentrations of TC, and the results are shown in Fig. 4A. The fluorescence spectra of the samples were obtained using our method, and the data demonstrate the ability of the method to quantify TC in a concentration-dependent manner. The maximum emission of Eu^{3+} at 615 nm gradually increased with the increase of the concentration of TC. Fig. 4B shows the corresponding graph, and Fig. 4C shows the calibration plot with a linear dynamic range of 20–320 nM ($Y = 5.04 \times 10^2 X + 4.67 \times 10^3$, $R^2 = 0.987$). The limit of detection (LOD) was estimated to be ~2.0 nM, which was calculated based on 3σ/slope. σ denotes the standard deviation of the blank sample, whereas the slope denotes the slope of the calibration curve. The LOD was lower than the MRL of TC regulated by the European Union (i.e., 225 nM) [38].

3.8. Naked eye detection

We also investigated the possibility of using the naked eye as the detection method for the samples containing TC because of the high sensitivity of our method. Fig. 5A shows the photographs of the samples containing TC with the concentration of 0–10 μM obtained after enrichment by our magnetic probes followed by Eu^{3+} sensing under the illumination of a UV lamp (λ_{max} = 365 nm). The fluorescence obtained from the sample containing TC with the concentration of 0.156 μM could be slightly distinguished from blank. After the samples stood for ~5 min, the precipitates resulting from the conjugates of the magnetic probe-TC-Eu^{3+} conjugates with pink emission were observed on the bottom of the vials with a concentration of TC above 0.156 μM (Fig. 5B). The results demonstrated that we could visualize the results of the samples containing TC with a concentration above ~0.156 μM using our approach. The lowest visible concentration was

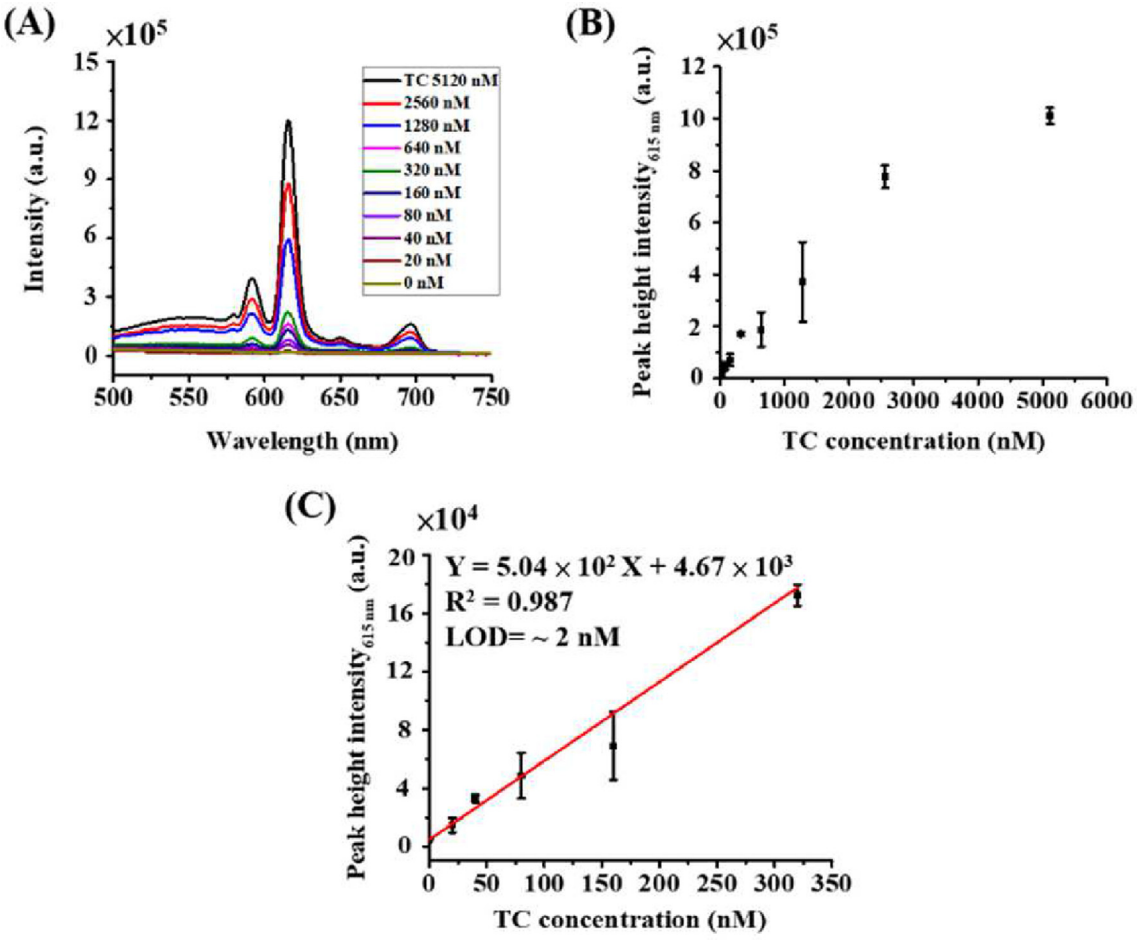

Fig. 4. (A) Fluorescence spectra of the samples containing TC (20–5120 nM) obtained by using the Gd^{3+} probes as the probes followed by adding Eu^{3+} (0.1 mM, 50 μL). (B) The corresponding plot by plotting the peak intensity at 615 nm versus TC concentration based on the results obtained in Panel (A). (C) The plot with the linear dynamic range obtained from Panel (B).

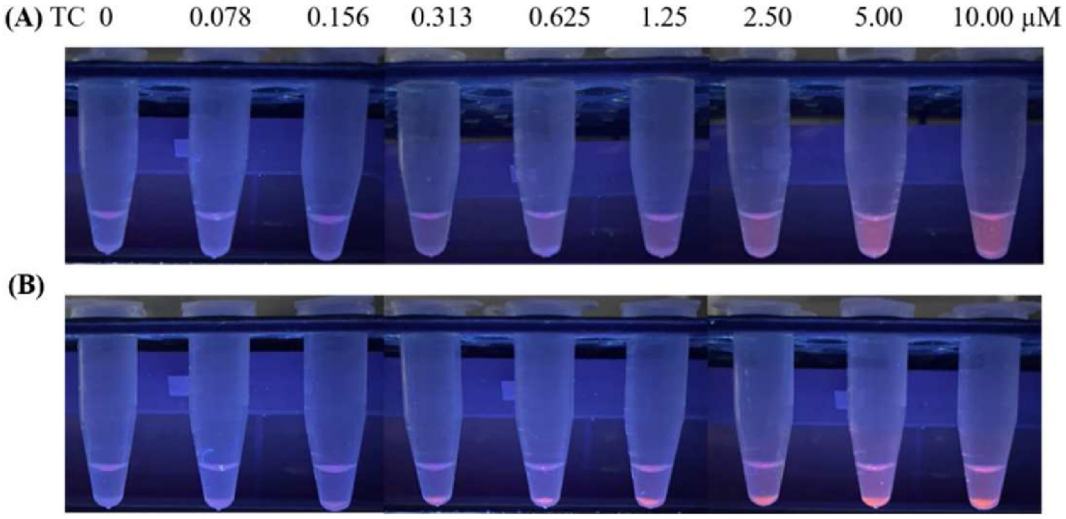

Fig. 5. Photographs of the sample (1 mL) containing TC (0–10 μM) obtained after using the Gd^{3+} conjugates as trapping probe followed by adding Eu^{3+}. The photographs were taken by a camera under a UV light (λ_{max} = 365 nm) obtained (A) before and (B) after standing for 5 min.

lower than that MRL of TC regulated by the European Union (i.e., 225 nM) [38], indicating the possibility of using the developed method for rapid screening of the presence of TC in aqueous samples.

3.9. Effects of interference species

The selectivity of our approach was investigated by spiking Na^{+}, K^{+}, Mg^{2+}, Ca^{2+}, Fe^{3+}, alanine, histidine, serine, and glucose to the samples containing TC. SI Fig. S9 [https://www.jfda-online.com/cgi/viewcontent.cgi?filename=0&article=3457&context=journal&type=additional] presents bar graphs summarizing the intensity at 615 nm obtained from the fluorescence spectra of the samples containing TC (100 nM) and the interference (1 μM) described earlier, as well as samples without TC. The data demonstrate the effectiveness of our method in distinguishing TC signals from interference signals, which is critical for accurate quantification in complex sample matrices. The fluorescence intensity of the resultant samples looked similar in the presence of those interference species (red bars). The presence of those interference species in the blank samples did not cause an apparent increase in the fluorescence background (blue bars). Although Mg^{2+}, Ca^{2+}, Fe^{3+} possess chelating capability with TC, the amount of Gd^{3+} in the probes was much higher than these metal ions in the sample, leading Gd^{3+} has a higher competitive power than other metal ions. These results suggested that the developed method was not affected too much by these selected interference species.

3.10. Examination of selectivity

To examine the selectivity of our method, we selected oxytetracycline (oxyTC) and penicillin as the model antibiotics. We prepared samples containing TC alone, mixtures of TC and oxyTC, or penicillin. The summarized results are shown in SI Fig. S10 [https://www.jfda-online.com/cgi/viewcontent.cgi?filename=0&article=3457&context=journal&type=additional]. The peak intensity at 615 nm was similar between the samples containing TC alone (marked as control) and the mixture of TC and penicillin (marked as penicillin) (blue bars). The structures of TC and penicillin are quite different, so it was not surprising to see that our method had good selectivity against TC in the mixture. This was also confirmed by the result from the sample containing penicillin alone (orange bar marked as penicillin), where the intensity at 615 nm was similar to that obtained from Tris buffer (orange bar marked as control). However, the peak intensity at 615 nm obtained from the sample containing TC (100 nM) and oxyTC (50 nM) was ~25% higher than that obtained from the control sample containing TC alone (blue bar marked as control). Additionally, the peak intensity at 615 nm (orange bar marked as oxyTC) derived from the sample containing only oxyTC was ~50% of the control (blue bar marked as control). Based on these results, our method can be used to detect the presence of oxyTC due to its similar structure and fluorescence feature to TC. However, it cannot be used to distinguish TC from oxyTC.

3.11. Evaluation and precision and accuracy

To determine the precision and accuracy of our method, a sample containing TC (50 nM) was used as the model sample. Multiple analyses were conducted, i.e. three times a day for four days. The concentrations of the samples were determined using the calibration curve shown in Fig. 4C, and the results are presented in SI Table S1 [https://www.jfda-online.com/cgi/viewcontent.cgi?filename=0&article=3457&context=journal&type=additional]. The precision and accuracy of the method were found to be 18.5% and 90.0%, respectively. The observed variations in the results could potentially be attributed to the variation of the amount of the probes used in each run, as the suspension of Gd^{3+}-Tris precipitates was used as the probes.

3.12. Analysis of the simulated real sample

A chicken broth sample spiked with TC (50 nM) was used as a simulated real sample and quantified by using the standard addition method to evaluate the feasibility of using our approach for the analysis of real-world samples. Fig. S11 [https://www.jfda-online.com/cgi/viewcontent.cgi?filename=0&article=3457&context=journal&type=additional] shows the resultant plot ($Y = 7.15 \times 10^2 X + 3.63 \times 10^4$, $R^2 = 0.967$) by plotting the fluorescence intensity at the wavelength of 615 nm versus the concentration of TC added in the samples. The concentration of TC in the sample was determined to be 50.8 nM, accordingly. The determined value was only ~1.6% different from the true value of 50 nM, indicating the suitability of using our approach to quantify TC from complex samples.

4. Conclusions

Although various magnetic probes have been developed for trapping TC, their fabrication methods are generally time-consuming and labor-

intensive. In this study, we have explored a new method for trapping TC using Gd^{3+} as the magnetic probe. When preparing Gd^{3+} in Tris buffer, the magnetic Gd^{3+}-Tris conjugates were readily formed and possessed selective trapping capacity against TC. The generation of the magnetic probes only took ~60 min. Using the developed probes to selectively trap TC from complex samples only took ~35 min because of the manipulable magnetism and good trapping efficiency. Moreover, we successfully used Eu^{3+} as the fluorescence sensing probe for the TC bound on the magnetic probe-TC conjugates. Eu^{3+} possessed good binding affinity with TC, whereas TC can enhance the fluorescence derived from Eu^{3+}. Generating our probes is much simpler and easier than other existing approaches. Our method can be used to detect TC derivatives, including oxyTC, which possess similar structures and fluorescence features to TC. However, it cannot be used to distinguish TC from oxyTC. Moreover, we believe that it is possible to further apply magnetic metal ions as probes to interact with other target species of interest if the target analytes have a specific binding affinity with the selected magnetic metal ions based on the HSAB theory. Such approaches not only possess a specific affinity for specific analytes but also can greatly reduce the time required for the fabrication of magnetic probes. Thus, we are optimistic about the future development of using magnetic metal ions as probes in the development of affinity-based analytic methods.

Conflict of interest

The authors declare that they do not have known competing financial interests or personal relationships that could have appeared to influence the report worked in this paper.

Acknowledgements

We thank the financial support of this study from the National Science and Technology Council, Taiwan (108–2113-M-009–018-MY3).

Appendix A. Supplementary data

Supplementary data to this article can be found online at https://doi.org/10.38212/2224-6614.3457.

References

[1] Nelson ML, Levy SB. The history of the tetracyclines. Ann N Y Acad Sci 2011;1241:17–32.
[2] Chopra I, Roberts M. Tetracycline Antibiotics: mode of action, applications, molecular biology, and epidemiology of bacterial resistance. Microbiol Mol Biol Rev 2001;65:232–60.
[3] Zakeri B, Wright GDWD. Chemical biology of tetracycline antibiotics. Biochem Cell Biol 2008;86:124–36.
[4] Daghrir R, Drogui P. Tetracycline antibiotics in the environment: a review. Environ Chem Lett 2013;11:209–27.
[5] Speer BS, Shoemaker NB, Salyers AA. Bacterial resistance to tetracycline: mechanisms, transfer, and clinical significance. Clin Microbiol Rev 1992;5:387–99.
[6] Chen F, Ying G-G, Kong L-X, Wang L, Zhao J-L, Zhou L-J, et al. Distribution and accumulation of endocrine-disrupting chemicals and pharmaceuticals in wastewater irrigated soils in Hebei, China. Environ Pollut 2011;159:1490–8.
[7] Wollenberger L, Halling-Sørensen B, Kusk KO. Acute and chronic toxicity of veterinary antibiotics to *Daphnia magna*. Chemosphere 2000;40:723–30.
[8] Liu X, Huang D, Lai C, Zeng G, Qin L, Zhang C, et al. Recent advances in sensors for tetracycline antibiotics and their applications. TrAC, Trends Anal Chem 2018;109:260–74.
[9] Baghani A, Mesdaghinia A, Rafieiyan M, Soltan Dallal MM, Douraghi M. Tetracycline and ciprofloxacin multiresidues in beef and chicken meat samples using indirect competitive ELISA. J Immunoassay Immunochem 2019;40:328–42.
[10] Cinquina AL, Longo F, Anastasi G, Giannetti L, Cozzani R. Validation of a high-performance liquid chromatography method for the determination of oxytetracycline, tetracycline, chlortetracycline and doxycycline in bovine milk and muscle. J Chromatogr A 2003;987:227–33.
[11] Zhou Q, Zhang Y, Wang N, Zhu L, Tang H. Analysis of tetracyclines in chicken tissues and dung using LC–MS coupled with ultrasound-assisted enzymatic hydrolysis. Food Control 2014;46:324–31.
[12] Xiong Y, Zhou H, Zhang Z, He D, He C. Molecularly imprinted on-line solid-phase extraction combined with flow-injection chemiluminescence for the determination of tetracycline. Analyst 2006;131:829–34.
[13] Li Y, Du Q, Zhang X, Huang Y. Ratiometric detection of tetracycline based on gold nanocluster enhanced Eu^{3+} fluorescence. Talanta 2020;206:120202.
[14] Han L, Fan YZ, Qing M, Liu SG, Yang YZ, Li NB, et al. Smartphones and test paper-assisted ratiometric fluorescent sensors for semi-quantitative and visual assay of tetracycline based on the target-induced synergistic effect of antenna effect and inner filter effect. ACS Appl Mater Interfaces 2020;12:47099–107.
[15] Wang C-Y, Wang C-C, Zhang X-W, Ren X-Y, Yu B, Wang P, et al. A new Eu-MOF for ratiometrically fluorescent detection toward quinolone antibiotics and selective detection toward tetracycline antibiotics. Chin Chem Lett 2022;33:1353–7.
[16] Li X, Fan K, Yang R, Du X, Qu B, Miao X, et al. A long lifetime ratiometrically luminescent tetracycline nanoprobe based on Ir(III) complex-doped and Eu^{3+}-functionalized silicon nanoparticles. J Hazard Mater 2020;386:121929.
[17] Yan Y, Liu JH, Li RS, Li YF, Huang CZ, Zhen SJ. Carbon dots synthesized at room temperature for detection of tetracycline hydrochloride. Anal Chim Acta 2019;1063:144–51.
[18] Li C, Zhu L, Yang W, He X, Zhao S, Zhang X, et al. Amino-functionalized Al–MOF for fluorescent detection of tetracyclines in milk. J Agric Food Chem 2019;67:1277–83.
[19] Yang X, Luo Y, Zhu S, Feng Y, Zhuo Y, Dou Y. One-pot synthesis of high fluorescent carbon nanoparticles and their applications as probes for detection of tetracyclines. Biosens Bioelectron 2014;56:6–11.
[20] Li C, Yang W, Zhang X, Han Y, Tang W, Yue T, et al. A 3D hierarchical dual-metal–organic framework heterostructure up-regulating the pre-concentration effect for ultrasensitive fluorescence detection of tetracycline antibiotics. J Mater Chem C 2020;8:2054–64.
[21] Valverde RS, García MDG, Galera MM, Goicoechea HC. Determination of tetracyclines in surface water by partial least squares using multivariate calibration transfer to correct the effect of solid phase preconcentration in photochemically induced fluorescence signals. Anal Chim Acta 2006;562:85–93.

[22] Şirin S, Clavero E, Salvadó J. Potential pre-concentration methods for *Nannochloropsis gaditana* and a comparative study of pre-concentrated sample properties. Bioresour Technol 2013;132:293–304.
[23] Duan M-L, Huang Y-M, Wu S-S, Li G-Q, Wang S-Y, Chen M-H, et al. Rapid and sensitive detection of *Salmonella enteritidis* by a pre-concentrated immunochromatographic assay in a large-volume sample system. RSC Adv 2013;7: 55141–7.
[24] Lian L, Lv J, Wang X, Lou D. Magnetic solid–phase extraction of tetracyclines using ferrous oxide coated magnetic silica microspheres from water samples. J Chromatogr A 2018;1534:1–9.
[25] Wang S-X, Ma R-R, Mazzu YZ, Zhang J-W, Li W, Tan L, et al. Specific adsorption of tetracycline from milk by using biocompatible magnetic molecular imprinting material and evaluation by ECD. Food Chem 2020;326:126969.
[26] Li X, Li C, Chen L. Preparation of multifunctional magnetic–fluorescent nanocomposites for analysis of tetracycline hydrochloride. New J Chem 2015;39:9976–82.
[27] Zhang Y, Mehedi HM, Rong Y, Liu R, Li H, Ouyang Q, et al. An upconversion nanosensor for rapid and sensitive detection of tetracycline in food based on magnetic-field-assisted separation. Food Chem 2022;373:131497.
[28] Wei J-L, Huang D-Y, Chen Y-C. Using gadolinium ions as affinity probes to selectively enrich and magnetically isolate bacteria from complex samples. Anal Chim Acta 2020;1113: 18–25.
[29] Wei J-L, Chen Y-C. Using magnetic ions to probe and induce magnetism of pyrophosphates, bacteria, and mammalian cells. ACS Appl Mater Interfaces 2018;10:30837–43.
[30] Pearson RG. Hard and soft acids and bases. J Am Chem Soc 1963;85:3533–9.
[31] Syamchand SS, Sony G. Europium enabled luminescent nanoparticles for biomedical applications. J Lumin 2015;165: 190–215.
[32] Hirsch LM, Van Geel TF, Winefordner JD, Kelly RN, Schulman SG. Characteristics of the binding of europium(III) to tetracycline. Anal Chim Acta 1985;166:207–19.
[33] Chen W-Y, Chen Y-C. MALDI MS analysis of oligonucleotides: desalting by functional magnetite beads using microwave-assisted extraction. Anal Chem 2007;79: 8061–6.
[34] Xie Y-Z, Shan G-G, Li P, Zhou Z-Y, Su Z-M. A novel class of Zn(II) Schiff base complexes with aggregation-induced emission enhancement (AIEE) properties: synthesis, characterization and photophysical/electrochemical properties. Dyes Pigments 2013;96:467–74.
[35] Babić S, Horvat AJM, Mutavdžić PD, Kaštelan-Macan M. Determination of pKa values of active pharmaceutical ingredients. TrAC, Trends Anal Chem 2007;26:1043–61.
[36] Huang C, Luo Y, Li J, Liu C, Zhou T, Deng J. pH-regulated H_4TCPE@Eu/AMP ICP sensor array and its fingerprinting on test papers: toward point-of-use systematic analysis of environmental antibiotics. Anal Chem 2021;93:9183–92.
[37] Georges J. Lanthanide-sensitized luminescence and applications to the determination of organic analytes. A review. Analyst 1993;118:1481–6.
[38] Luo Y, Xu J, Li Y, Gao H, Guo J, Shen F, et al. A novel colorimetric aptasensor using cysteamine-stabilized gold nanoparticles as probe for rapid and specific detection of tetracycline in raw milk. Food Control 2015;54:7–15.